CONFIDENTIAL

Copy
RM L54L03b

335

NACA RM L54L03b

NACA

RESEARCH MEMORANDUM

LIFT, DRAG, AND STATIC LONGITUDINAL STABILITY DATA FROM AN EXPLORATORY INVESTIGATION AT A MACH NUMBER OF 6.86 OF AN AIRPLANE CONFIGURATION HAVING A WING OF TRAPEZOIDAL PLAN FORM

By Jim A. Penland, Herbert W. Ridyard,
and David E. Fetterman, Jr.

Langley Aeronautical Laboratory
Langley Field, Va.

CLASSIFIED DOCUMENT

This material contains information affecting the National Defense of the United States within the meaning of the espionage laws, Title 18, U.S.C., Secs. 793 and 794, the transmission or revelation of which in any manner to an unauthorized person is prohibited by law.

NATIONAL ADVISORY COMMITTEE
FOR AERONAUTICS

WASHINGTON
January 18, 1955

CONFIDENTIAL

NATIONAL ADVISORY COMMITTEE FOR AERONAUTICS

RESEARCH MEMORANDUM

LIFT, DRAG, AND STATIC LONGITUDINAL STABILITY DATA FROM AN EXPLORATORY INVESTIGATION AT A MACH NUMBER OF 6.86 OF AN AIRPLANE CONFIGURATION HAVING A WING OF TRAPEZOIDAL PLAN FORM

By Jim A. Penland, Herbert W. Ridyard, and David E. Fetterman, Jr.

SUMMARY

An investigation to determine the lift, drag, and static longitudinal stability characteristics of an airplane configuration having a trapezoidal wing with modified hexagonal airfoil section and 5° semiangle wedge tail sections has been carried out in the Langley 11-inch hypersonic tunnel. The tests were made at a Mach number of 6.86 and Reynolds numbers of 343,000 and 566,000 based on wing mean aerodynamic chord. Data were obtained for angles of attack up to about 28° for the complete airplane configuration and up to about 14° for the body alone, the body-wing configuration, and the body-tail configuration.

INTRODUCTION

The aircraft configurations previously investigated experimentally at hypersonic speeds have been restricted mainly to missile types which were not required to be able to land and which, therefore, had relatively small wings or wings of very low aspect ratio. The purpose of the present investigation was to determine the characteristics of a configuration conforming more closely to a piloted aircraft having a wing area sufficient for conventional landing. Of the various possible configurations, one was selected for this exploratory study which was expected to have satisfactory low-speed characteristics and satisfactory transonic characteristics. This configuration (fig. 1) employs a trapezoidal wing and the arrangement, in general, is similar to conventional airplanes. Two particular features were incorporated which are believed to be desirable for hypersonic operation - relatively large leading-edge radii for both wing and tail, and wedge-shaped sections for the tail surfaces. The large leading-edge radius is essential in order to keep the heat-transfer rates

within feasible limits, and the wedge tail sections were selected to provide the desired tail effectiveness with tail surfaces of conventional size (ref. 1).

Six-component data have been obtained both for the complete airplane configuration and for the various components tested. This report presents the lift, drag, and pitching-moment data with a minimum of analysis in order to expedite release of this information.

SYMBOLS

C_L	lift coefficient, L/qS
C_D	drag coefficient, D/qS
L/D	lift-drag ratio, C_L/C_D
C_m	pitching-moment coefficient, nose-up moment positive, $M'/qS\bar{c}$, moment reference at 54 percent of the wing mean aerodynamic chord
C_N	normal-force coefficient, N/qS
x_{cp}	distance from nose to center of pressure, percent body length
$\frac{\partial C_m}{\partial C_N}$	rate of change of pitching-moment coefficient with normal force coefficient
L	lift
D	drag
M'	pitching moment
N	normal force
q	free-stream dynamic pressure
S	total wing area including body intercept
l	body length, in.
c	wing chord
$\bar{c}$	wing mean aerodynamic chord

c_t tail chord

M Mach number

R Reynolds number based on wing mean aerodynamic chord

α angle of attack measured between body center line and relative wind, deg

MODELS AND APPARATUS

Models

The models used for the present tests consisted of a complete model (fig. 1), a body alone, a body-wing combination, and a body-tail combination. Details concerning the airplane model are given in the three-view drawing (fig. 2), in the sketches of the airfoil sections (fig. 3), and in the table of geometric characteristics (table I). The wing and tail sections were designed with large leading-edge radii because of heat-transfer considerations at high Mach numbers. The wing leading-edge radius, for example, would be approximately 1.5 inches at the wing-fuselage intersection for a full-size airplane having a wing span of about 28 feet. Inasmuch as the effectiveness of lifting surfaces having a flat plate or conventional airfoil sections decreases considerably with Mach number at high supersonic speeds (ref. 1), the effectiveness of tail surfaces of conventional size utilizing these airfoil sections would be marginal or insufficient at the Mach number of the present tests. Several types of tail airfoil sections therefore are being considered and the present results were obtained with a 5° semiangle wedge section. A photograph of the complete model configuration installed in the Langley 11-inch hypersonic tunnel (M = 6.86 nozzle) may be seen in figure 4.

Wind Tunnel

The tests were conducted in the Langley 11-inch hypersonic blowdown tunnel. This tunnel is equipped with a single-step two-dimensional nozzle constructed of Invar. The nozzle is designed by the method of characteristics with a correction made for boundary layer and operates at an average Mach number of 6.86. The duration of each run was about 80 seconds, and the variation of test section Mach number with time is negligible after the first 15 seconds of running time. This constant Mach number flow made it possible to obtain forces for several angles of attack during each run. The model was held at low angles of attack for starting and stopping the runs in order to minimize shock loads on the strain-gage balance which supports the model. Further details concerning the 11-inch tunnel installation may be found in reference 2.

Strain-Gage Force Balances

Six-component force and moment measurements were made by means of two strain-gage balances. Five components, including normal force, side force, pitching moment, rolling moment, and yawing moment were measured on a balance mounted inside the model. The sixth component, chord force, was obtained on a two-component external balance measuring normal force and chord force. The model was attached to the balance and the variation of angle of attack was accomplished by rotating the balance and model through the desired angle, thus keeping constant geometry between model and balance for all conditions.

Schlieren System

An off-axis, single-pass, two-mirror, schlieren system utilizing a mercury-vapor light source was used for all tests. Schlieren photographs were recorded on standard panchromatic film exposed for approximately 3 microseconds. These photographs were obtained at each test point and were used to measure the angle of attack of the model for all tests. The accuracy with which the angles of attack were measured was within 0.10°.

TESTS

Tests were made at stagnation pressures of 20 and 33 atmospheres absolute. The stagnation temperature was maintained at an average value of 675° F to avoid air liquefaction (ref. 3). These conditions correspond to Reynolds numbers of 343,000 and 566,000 based on the mean aerodynamic chord of the wing. The absolute humidity was kept to less than 1.87×10^{-5} pounds of water vapor per pound of dry air for all tests. Because of the load limitations of the five-component balance used, some of the present tests were conducted at the reduced stagnation pressure. The pitching-moment and center-of-pressure data therefore were obtained for the complete airplane and its components at the lower Reynolds number of 343,000. Lift and drag data were obtained for the complete airplane and its components at a Reynolds number of 566,000. Lift and drag data were also obtained for the complete airplane at a Reynolds number of 343,000 for comparison purposes.

Lift, drag, and pitching moment were obtained for angles of attack up to about 28° for the complete airplane configuration and up to about 14° for the body-alone, body-wing, and body-tail configurations.

SUMMARY OF RESULTS

The experimental aerodynamic characteristics of the models are tabulated for each angle of attack in table II. The variations with angle of attack of the aerodynamic characteristics, C_L, C_D, L/D, C_m, and x_{cp} for the complete airplane configuration and its components are presented in figure 5 at a Mach number of 6.86 for Reynolds numbers of 343,000 and 566,000. As noted previously, lift and drag tests were made at both Reynolds numbers only for the complete airplane. The results of these tests which are presented in figure 5(a) show little effect of Reynolds number on C_L and C_D; however, a small increase in maximum L/D with increasing Reynolds number is indicated. In figure 5 the test data show very little scatter; however, some erratic tendencies are shown for the variations of center of pressure at angles of attack lower than 5° at which considerable scatter in the data resulted from inaccuracies in the measurement of the small quantities. In figure 6 typical schlieren photographs are shown of the complete model at various angles of attack. Schlieren photographs of the body-wing, body-tail, and body-alone configurations are shown in figure 7.

The effect of the components of the airplane on the aerodynamic characteristics are presented in figures 8 to 12. As expected at hypersonic speeds, a large portion of the lift of the complete model (30 percent) is contributed by the body alone. (See fig. 8.) The greater portion of the remaining lift is contributed by the wing. The lift contributed by the tail is considerably greater at higher angles of attack when the tail is combined with the body than when the tail is combined with the body and wing.

In figure 9 it may be seen that at angles of attack near zero, the drag of the body-wing and body-tail configurations are the same, indicating that the drag contributed by the wing and the tail are about equal. Furthermore, it appears that the drag of the body, the wing, and the tail each contributed approximately the same proportion of the total minimum drag.

The maximum measured value of the lift-drag ratio of the complete model was 2.36 at a Reynolds number of 566,000. Contributing factors to this relatively low lift-drag ratio were the blunt leading-edges and high-drag wedge tail sections.

In figure 11 the curves for the complete model and body-tail configuration show a stable variation of pitching-moment coefficient with angle of attack, whereas those for the body and body-wing configurations show an unstable variation.

The variations of center of pressures for the four configurations (fig. 12) indicate small rearward movements with angle of attack, with the complete model having the more nearly constant trend with α.

The large contribution of the horizontal tail surfaces to the static longitudinal stability of the model may be seen from the curves of figure 13, which show the variation of the pitching-moment coefficient with normal-force coefficient for the complete model and for the body-wing combination.

The variation of the static-longitudinal-stability parameter $\partial C_m/\partial C_N$ with normal-force coefficient for the complete model and the body-wing configuration is presented in figure 14. For the complete model $\partial C_m/\partial C_N$ varies from about -0.14 at $C_N = 0.1$ to about -0.30 at $C_N = 0.8$. Below $C_N = 0.1$ the curve exhibits the unusual tendency of becoming more negative with decreasing C_N. This tendency follows from the reversal of curvature of the pitching-moment variation with normal force shown in figure 13. A comparison of the curves of figure 14 shows that there is a constant difference between the curves of the body-wing configuration and the complete model equal to about $0.25\ \partial C_m/\partial C_N$ for values of C_N above 0.1. This constant difference corresponds to a movement of the neutral point between the body-wing configuration and the complete model of approximately 25 percent of the wing mean aerodynamic chord and represents the tail contribution to the longitudinal stability parameter $\partial C_m/\partial C_N$.

Langley Aeronautical Laboratory,
National Advisory Committee for Aeronautics,
Langley Field, Va., December 1, 1954.

REFERENCES

1. McLellan, Charles H.: A Method for Increasing the Effectiveness of Stabilizing Surfaces at High Supersonic Mach Numbers. NACA RM L54F21, 1954.

2. McLellan, Charles H., Williams, Thomas W., and Bertram, Mitchel H.: Investigation of a Two-Step Nozzle in the Langley 11-Inch Hypersonic Tunnel. NACA TN 2171, 1950.

3. McLellan, Charles H., Williams, Thomas W.: Liquefaction of Air in the Langley 11-Inch Hypersonic Tunnel. NACA TN 3302, 1954.

TABLE I.- GEOMETRIC CHARACTERISTICS OF MODEL

Wing:	
Area (including area submerged in fuselage), sq. in.	6.24
Span, in.	4.33
Mean aerodynamic chord, in.	1.713
Root chord, in.	2.53
Tip chord, in.	0.354
Airfoil section	hexagonal with round leading edge
Taper ratio	0.140
Aspect ratio	3.00
Sweep of leading edge, deg	38.83
Sweep of c/4 line, deg	29
Incidence at fuselage center line, deg	0
Dihedral, deg	0
Geometric twist, deg	0
Horizontal and vertical tails:	
Area (including area submerged in fuselage), sq in.	2.06
Span, in.	2.69
Mean aerodynamic chord, in.	0.853
Root chord, in.	1.214
Tip chord, in.	0.317
Airfoil section	5° semiangle wedge
Taper ratio	0.261
Aspect ratio	3.52
Sweep of leading edge, deg	22.63
Dihedral, deg	0
Fuselage:	
Length, in.	7.50
Maximum diameter, in.	0.790
Fineness ratio	9.50
Base diameter, in.	0.790
Distance from nose to moment reference	3.950
Ogive nose length, in.	2.29
Ogive radius, in.	6.85

TABLE II.- AERODYNAMIC CHARACTERISTICS OF THE MODEL AND ITS COMPONENTS AT M = 6.86

(a) Two-Component Balance Data

α, deg	C_L	C_D	L/D	α, deg	C_L	C_D	L/D	α, deg	C_L	C_D	L/D
Complete model; R = 343,000											
0.21	0.0038	0.0392	0.097	7.38	0.132	0.0689	1.91	14.63	0.31	0.145	2.15
1.36	.0205	.0398	.514	8.40	.154	.0749	2.06	14.66	.313	.143	2.20
2.31	.0384	.0408	.941	8.45	.158	.0757	2.09	16.75	.385	.182	2.11
3.36	.0455	.0440	1.04	8.46	.163	.0755	2.16	16.81	.382	.177	2.16
4.40	.0622	.0473	1.32	9.43	.177	.0829	2.13	18.85	.461	.227	2.03
5.41	.0820	.0512	1.60	10.45	.202	.0924	2.18	21.06	.539	.283	1.90
6.41	.111	.0625	1.77	10.46	.201	.0903	2.23	21.13	.537	.287	1.87
6.43	.110	.0619	1.78	12.61	.253	.114	2.22	23.16	.623	.348	1.79
6.48	.116	.0616	1.89	12.63	.260	.118	2.21	25.38	.714	.427	1.67
								27.51	.80	.514	1.56
Complete model; R = 566,000											
0.30	0.0023	0.0365	0.062	4.36	0.0764	0.0490	1.56	8.51	0.1575	0.0694	2.26
1.28	.0189	.0383	.493	5.43	.0933	.0574	1.63	8.58	.1629	.0724	2.25
2.25	.0389	.0422	.922	6.33	.1133	.0589	1.92	10.66	.2167	.0919	2.36
2.28	.0384	.0415	.925	6.45	.1127	.0568	1.98	12.95	.2701	.1164	2.32
3.33	.0579	.0468	1.24	7.35	.1317	.0697	1.89	15.01	.3321	.1456	2.28
4.35	.0750	.0507	1.48								
Body alone; R = 566,000											
0.08	-0.0008	0.0139	-0.0609	6.16	0.0299	0.0205	1.46	10.20	0.0616	0.0307	2.01
2.08	.0078	.0152	.514	8.21	.0436	.0252	1.73	12.31	.0793	.0368	2.15
4.06	.0181	.0166	1.08	8.23	.0453	.0234	1.94	14.28	.0976	.0453	2.15
Body-tail; R = 566,000											
0.18	-0.0001	0.0284	-0.0031	6.23	0.0564	0.0374	1.510	10.30	0.0983	0.0557	1.760
2.21	.0180	.0298	.604	8.21	.0759	.0453	1.680	12.65	.1234	.0664	1.860
4.25	.0360	.0326	1.100	8.30	.0728	.0458	1.590	14.48	.1534	.0807	1.900
Body-wing; R = 566,000											
0.13	0.0041	0.025	0.162	6.31	0.0828	0.0420	1.97	10.60	0.1741	0.0686	2.54
2.23	.0302	.0315	.959	8.36	.1251	.0531	2.36	12.68	.2197	.0871	2.52
4.35	.0606	.0351	1.73	8.36	.1317	.0531	2.48	14.76	.2806	.1144	2.45

TABLE II.- AERODYNAMIC CHARACTERISTICS OF THE MODEL AND ITS COMPONENTS AT M = 6.86 – Concluded

(b) Five-Component Balance Data

α, deg	C_N	C_m	x_{cp}, percent l	α, deg	C_N	C_m	x_{cp}, percent l	α, deg	C_N	C_m	x_{cp}, percent l
Complete model; R = 343,000											
0	0.0046	-0.0002	51.7	1.98	0.0247	-0.0089	60.9	9.83	0.2152	-0.0403	57.0
0	.0064	-.0005	54.5	2.83	.0421	-.0123	59.4	14.78	.3663	-.0749	57.4
.04	.0013	-.0005	44.0	3.83	.0579	-.0146	58.4	19.75	.5735	-.1311	57.9
.96	.0065	-.0047	69.2	4.88	.0765	-.0172	57.8	24.70	.8183	-.2040	58.4
Body alone; R = 343,000											
0.02	------	0.0008	----	5.98	0.0374	0.0198	40.6	17.98	0.1382	0.0389	46.3
1.05	0.0038	.0057	18.5	7.97	.0490	.0247	41.2	20.03	.1685	.0391	47.4
1.93	.0167	.0091	40.3	9.97	.0631	.0289	42.3	21.93	.2003	.0393	48.2
2.95	.0179	.0124	36.9	11.90	.0839	.0322	43.9	23.95	.2288	.0395	48.8
4.00	.0179	.0149	33.7	13.93	.0999	.0349	44.7	25.90	.2621	.0397	49.2
5.02	.0245	.0174	36.5	16.00	.1135	.0378	45.1	27.95	.3028	.0399	49.7
Body-tail; R = 343,000											
0.12	0.0002	-0.0008	38.7	5.92	0.0545	-0.0205	61.3	17.68	0.2460	-0.1151	63.4
1.08	.0088	-.0037	62.3	7.88	.0767	-.0285	61.2	19.55	.2893	-.1411	63.8
2.02	.0163	-.0069	62.4	9.83	.1020	-.0388	61.4	21.50	.3347	-.1671	64.1
3.03	.0240	-.0099	62.1	11.87	.1290	-.0512	61.8	23.40	.3778	-.1923	64.3
3.98	.0345	-.0133	61.5	13.82	.1609	-.0678	62.3	25.35	.4287	-.2214	64.5
4.98	.0438	-.0170	61.6	15.70	.2030	-.0897	62.8	27.30	.4820	-.2505	64.6
Body-wing; R = 343,000											
0.05	0	0.0012	----	3.01	0.0444	0.0096	47.8	12.18	0.2011	0.0311	49.2
.06	0	.0005	----	3.93	.0642	.0133	48.0	14.23	.2590	.0339	49.7
.95	.0155	.0043	47.5	4.98	.0588	.0131	47.6	16.03	.3227	.0348	50.2
.96	.0117	.0038	45.3	6.05	.0706	.0192	46.5	18.13	.3898	.0348	50.7
2.03	.0289	.0068	47.3	8.06	.1092	.0241	47.7	20.12	.4698	.0342	51.0
2.15	.0325	.0072	47.6	10.10	.1539	.0283	48.5	25.13	.6801	.0263	51.8
3.00	.0471	.0104	47.7								

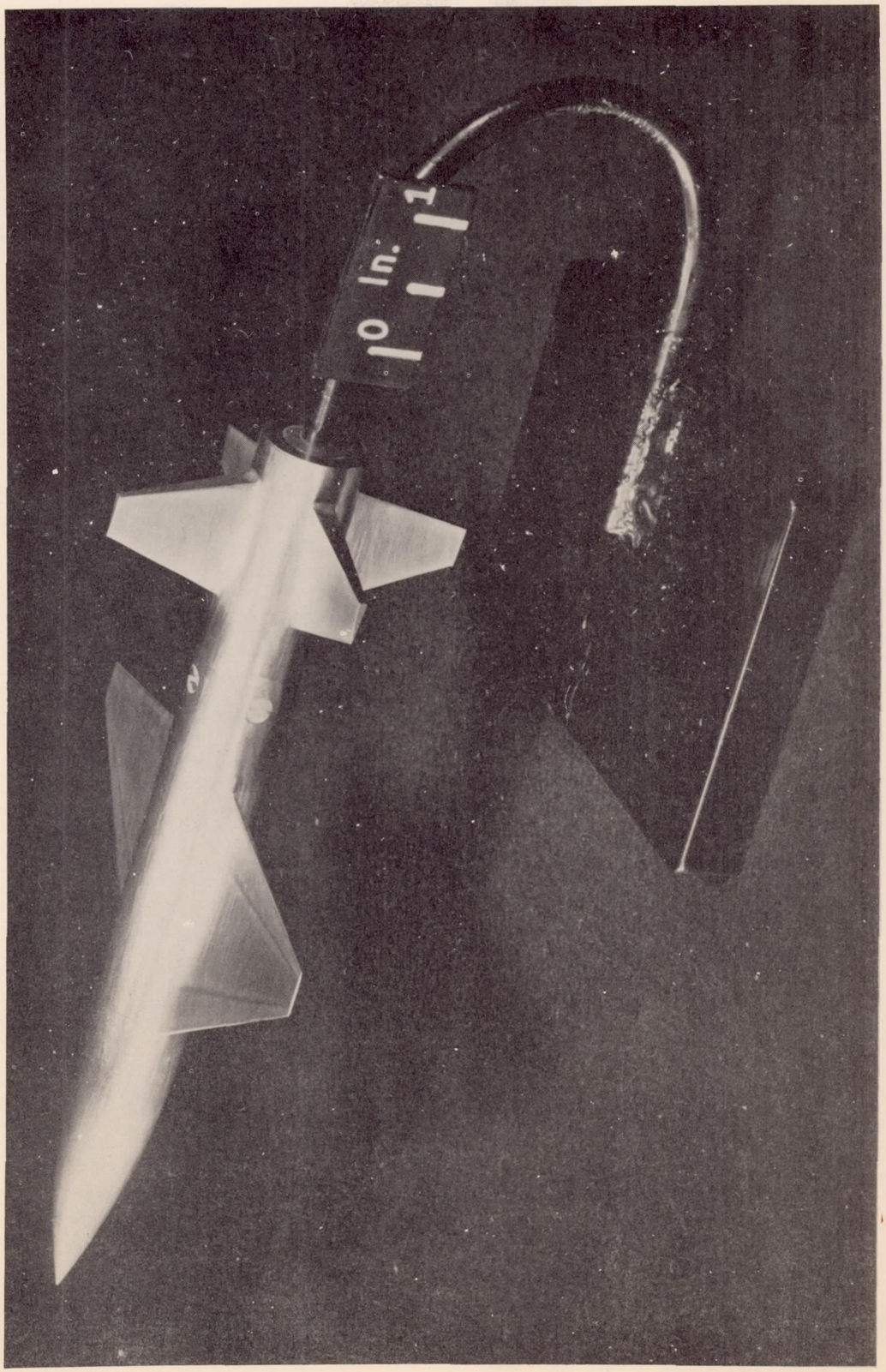

L-86688

Figure 1.- Photograph of complete model.

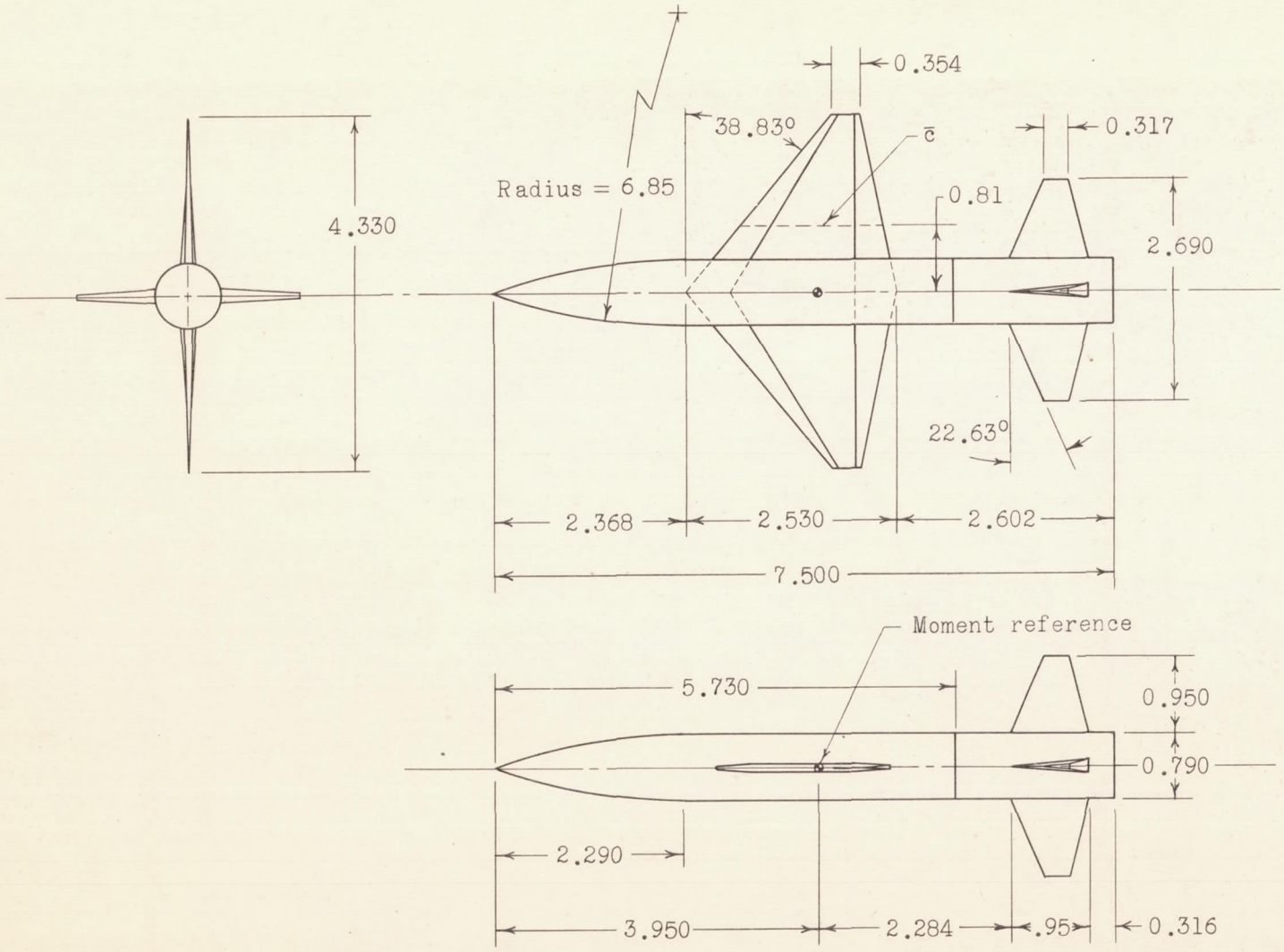

Figure 2.- Three-view sketch of wind-tunnel model. All dimensions in inches.

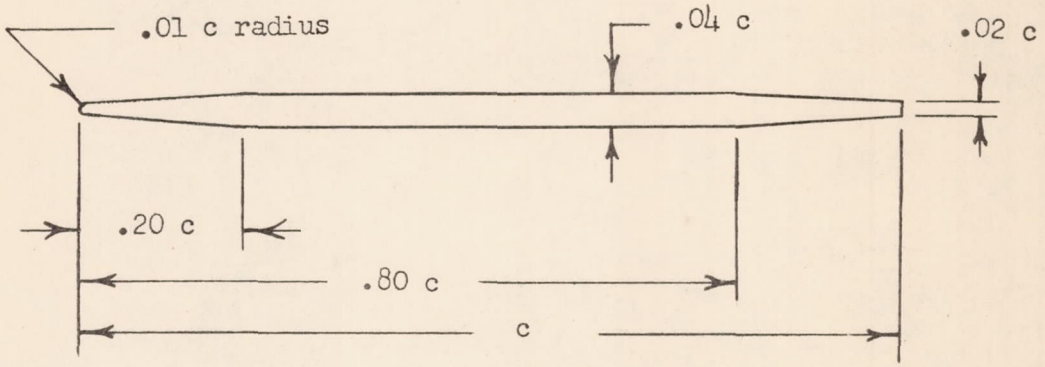

(a) Wing.

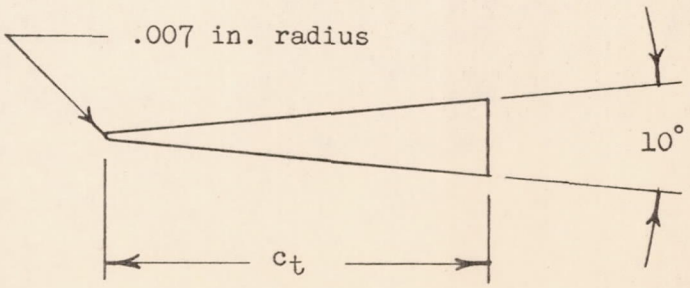

(b) Horizontal and vertical tails.

Figure 3.- Wing and tail airfoil sections used on model.

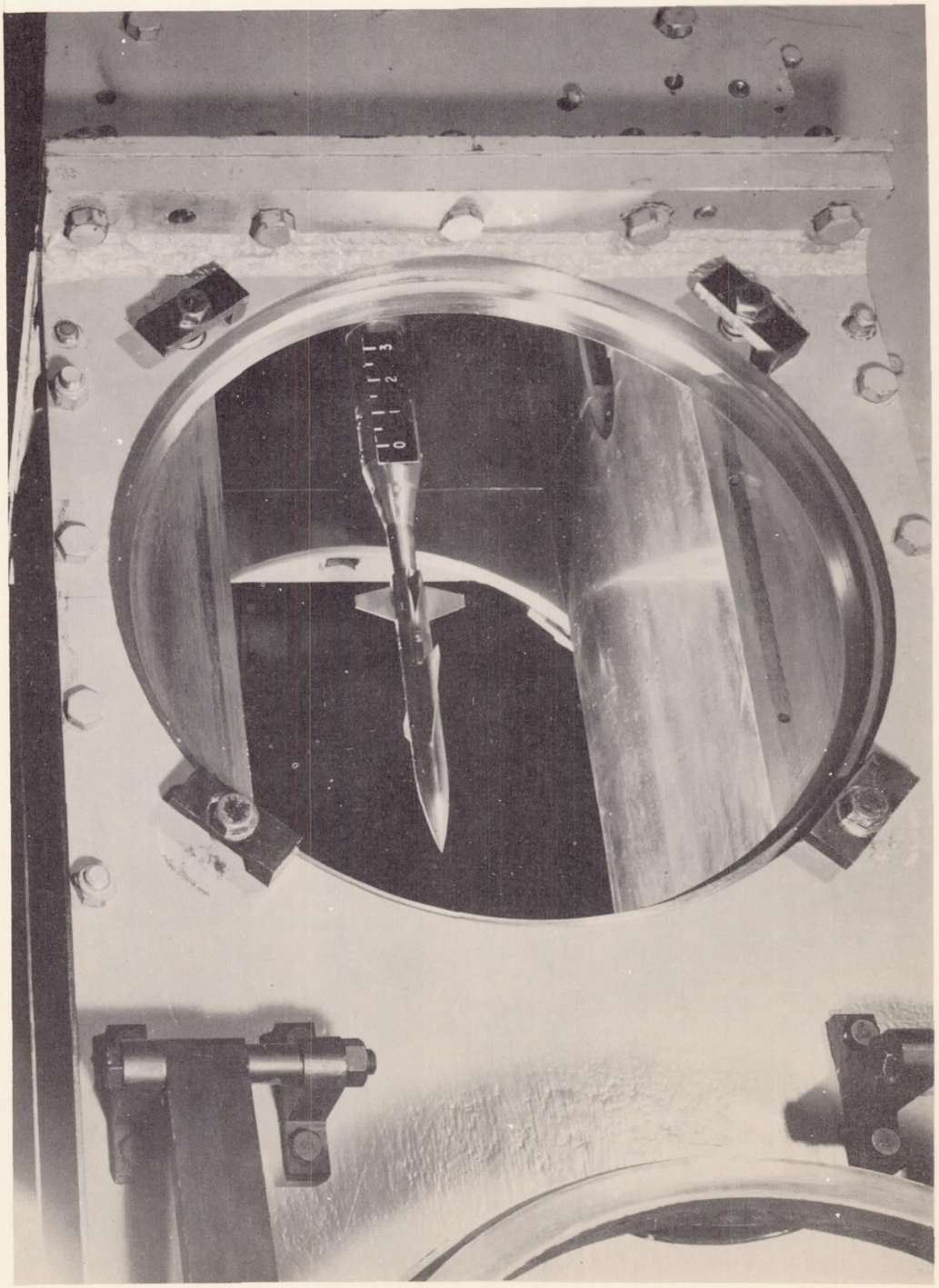

L-86712

Figure 4.- Installation of model in the Langley 11-inch hypersonic tunnel.

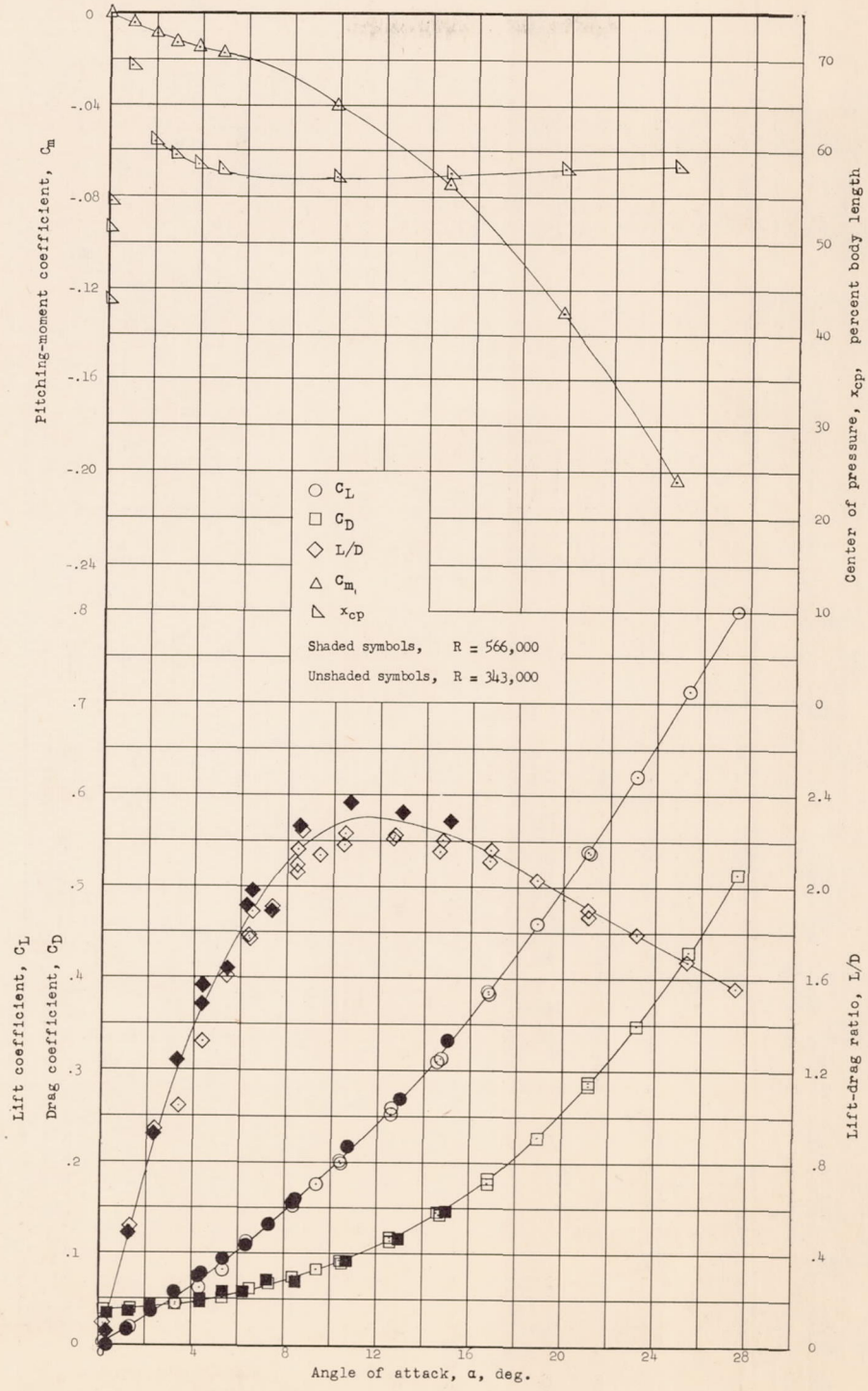

(a) Complete model.

Figure 5.- Experimental variations of the longitudinal characteristics of the model and its components with angle of attack. M = 6.86.

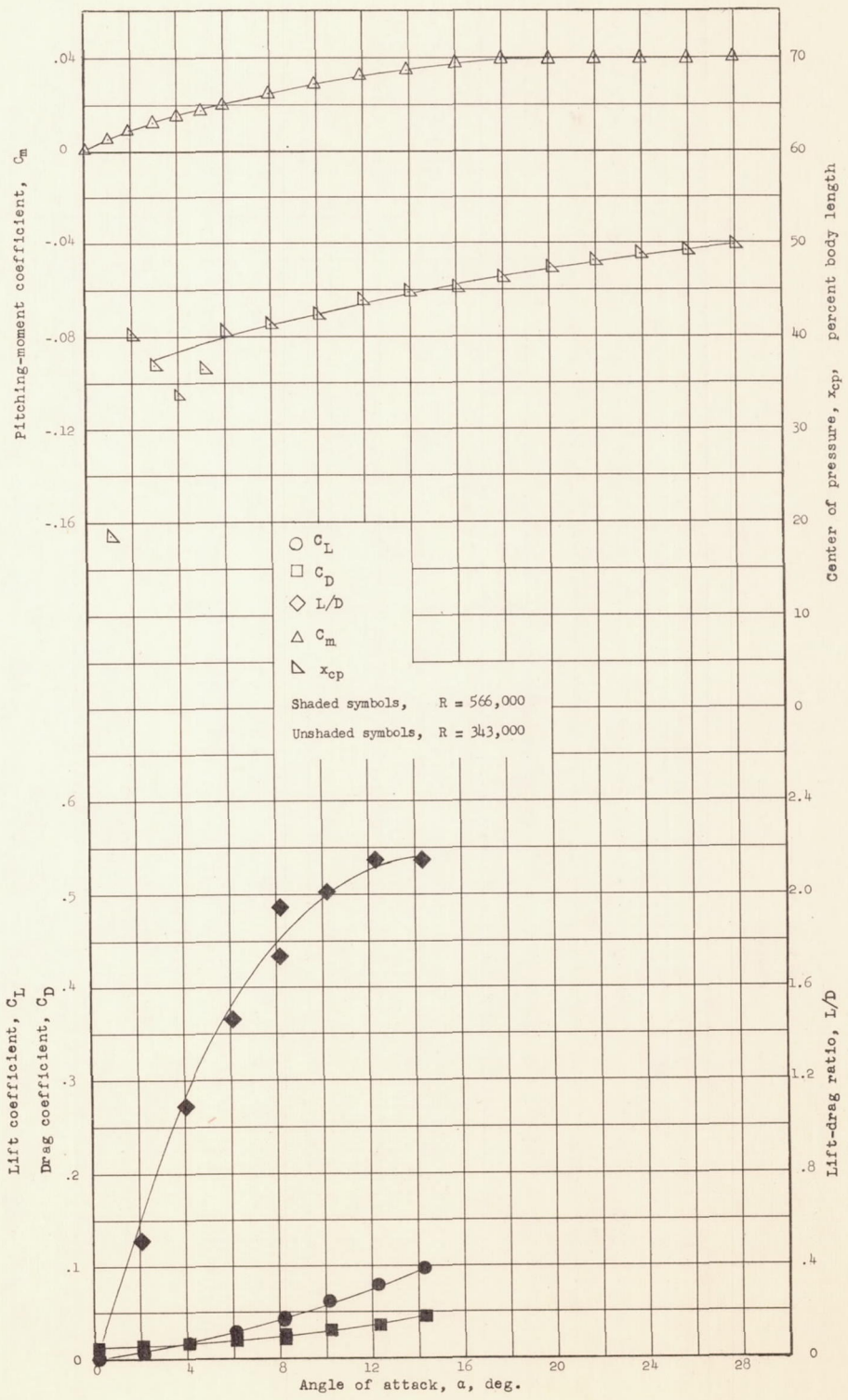

(b) Body alone.

Figure 5.- Continued.

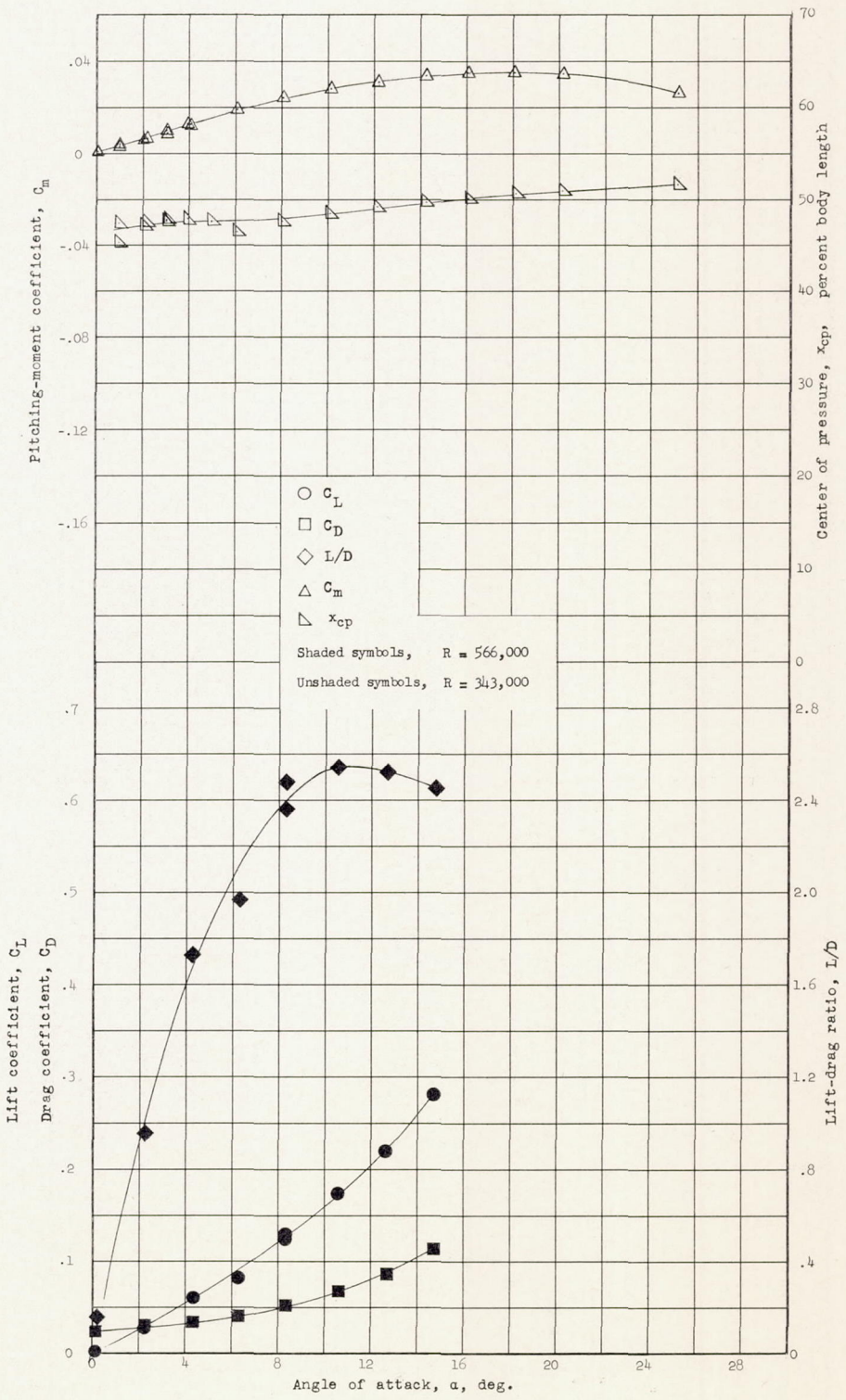

(c) Body-wing configuration.

Figure 5.- Continued.

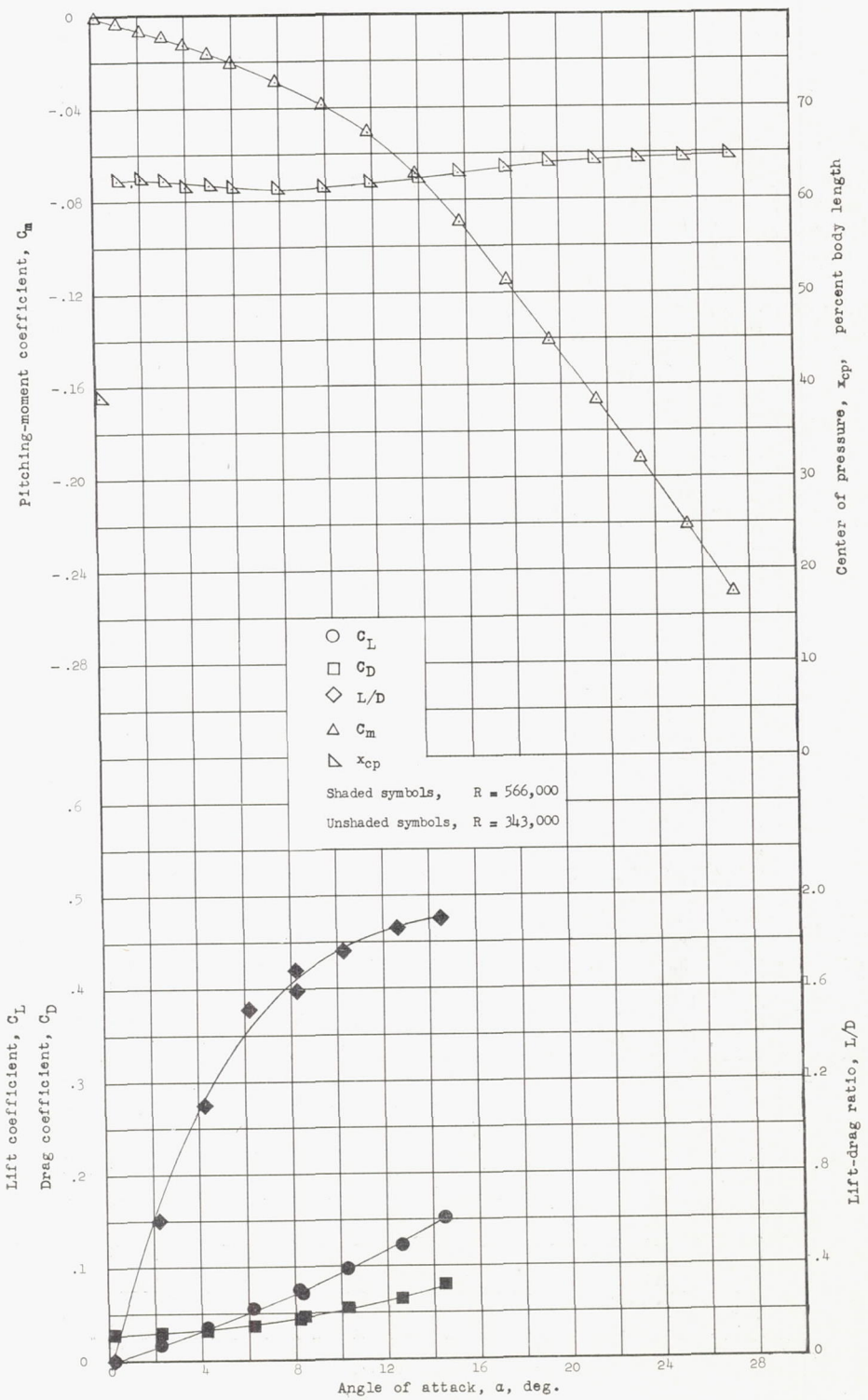

(d) Body-tail configuration.

Figure 5.- Concluded.

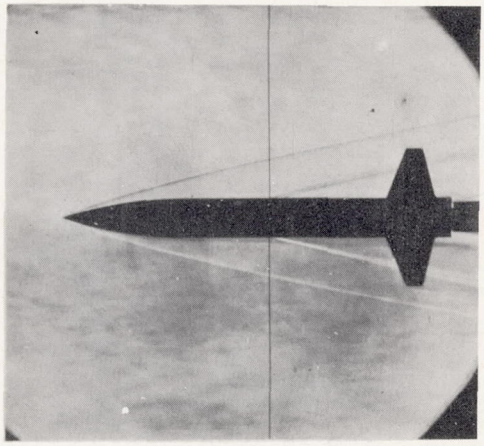

$\alpha = 0°$

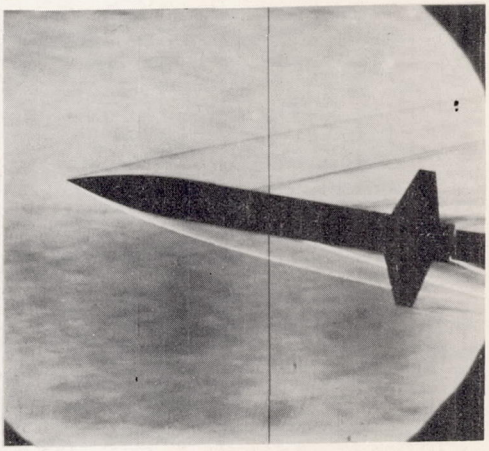

$\alpha = 10°$

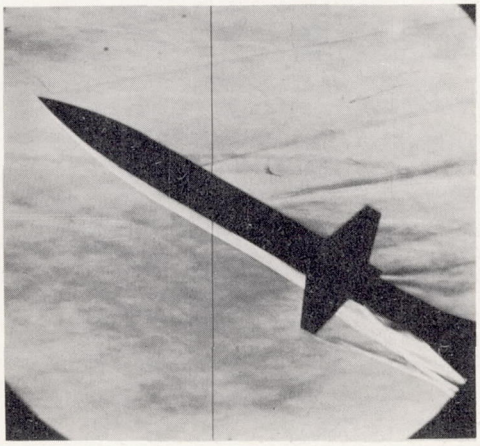

$\alpha = 30°$

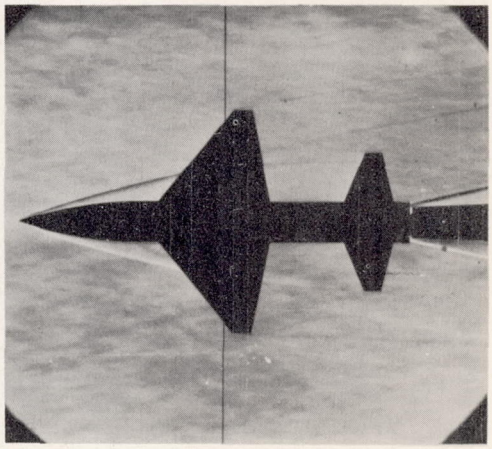

$\alpha = 0°$

L-86488

Figure 6.- Typical schlieren photographs of complete-model configuration.

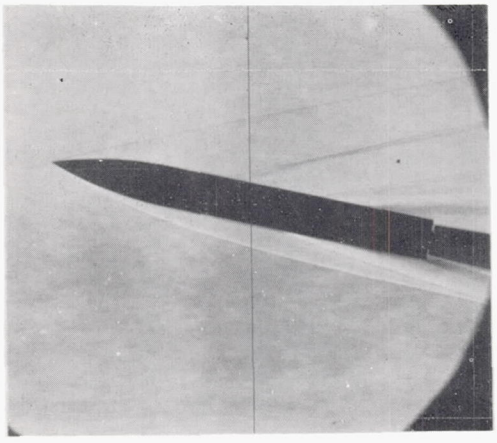

Body-wing configuration; $\alpha = 10^{\circ}$

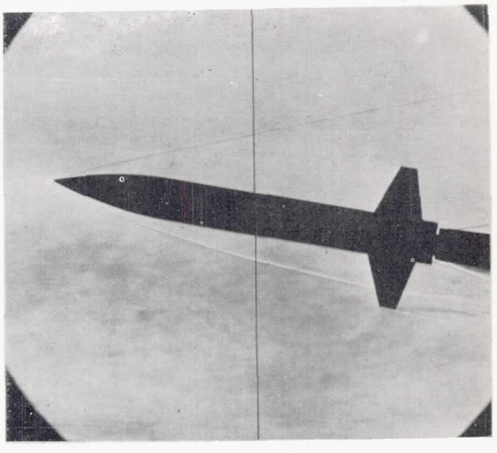

Body-tail configuration; $\alpha = 10^{\circ}$

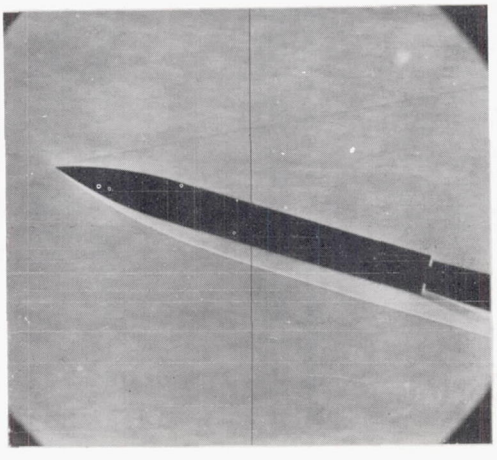

Body-alone configuration; $\alpha = 16^{\circ}$

L-86489

Figure 7.- Typical schlieren photographs of the body-wing, body-tail, and body-alone configurations.

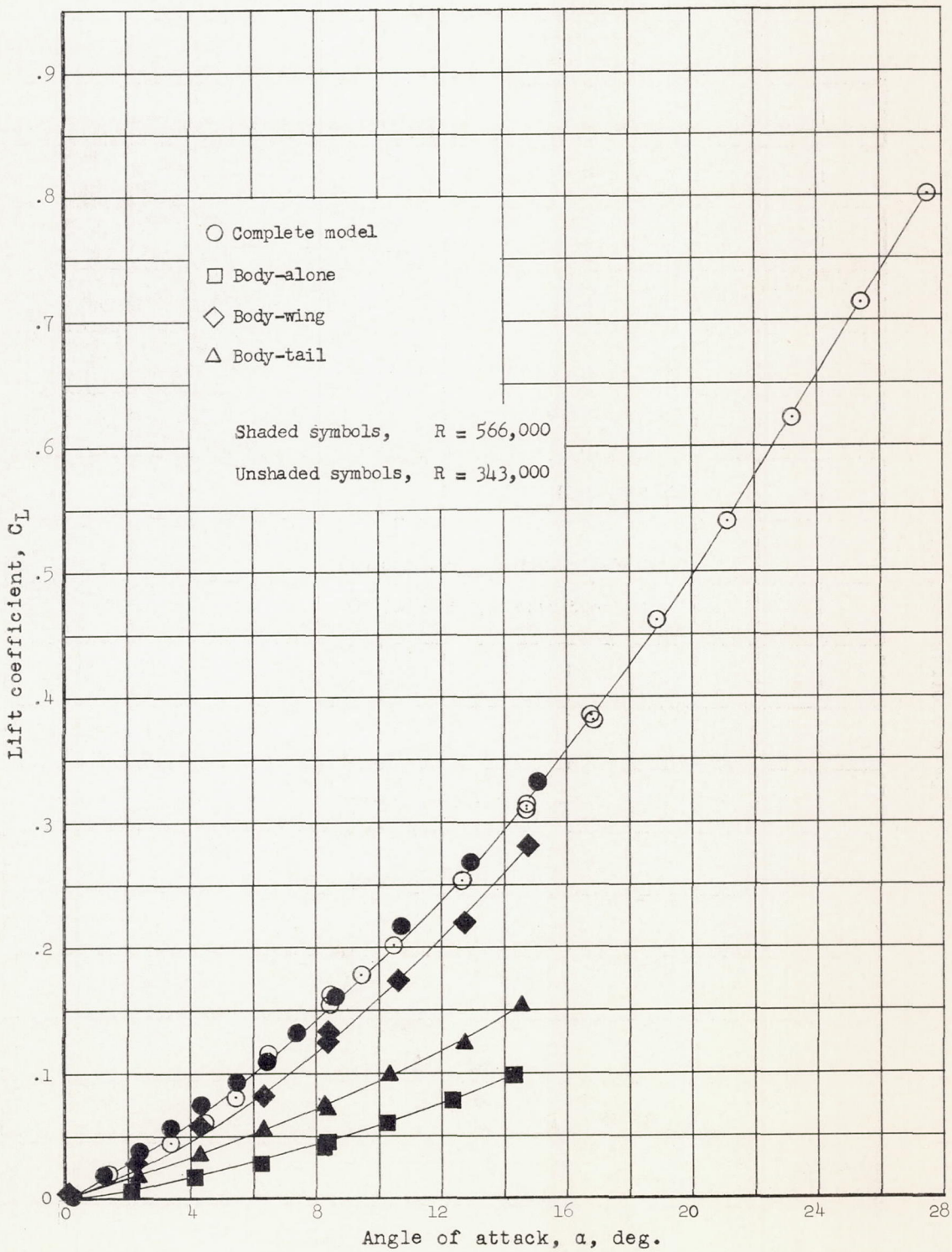

Figure 8.- The variations of the lift coefficient with angle of attack for the model and its components. M = 6.86.

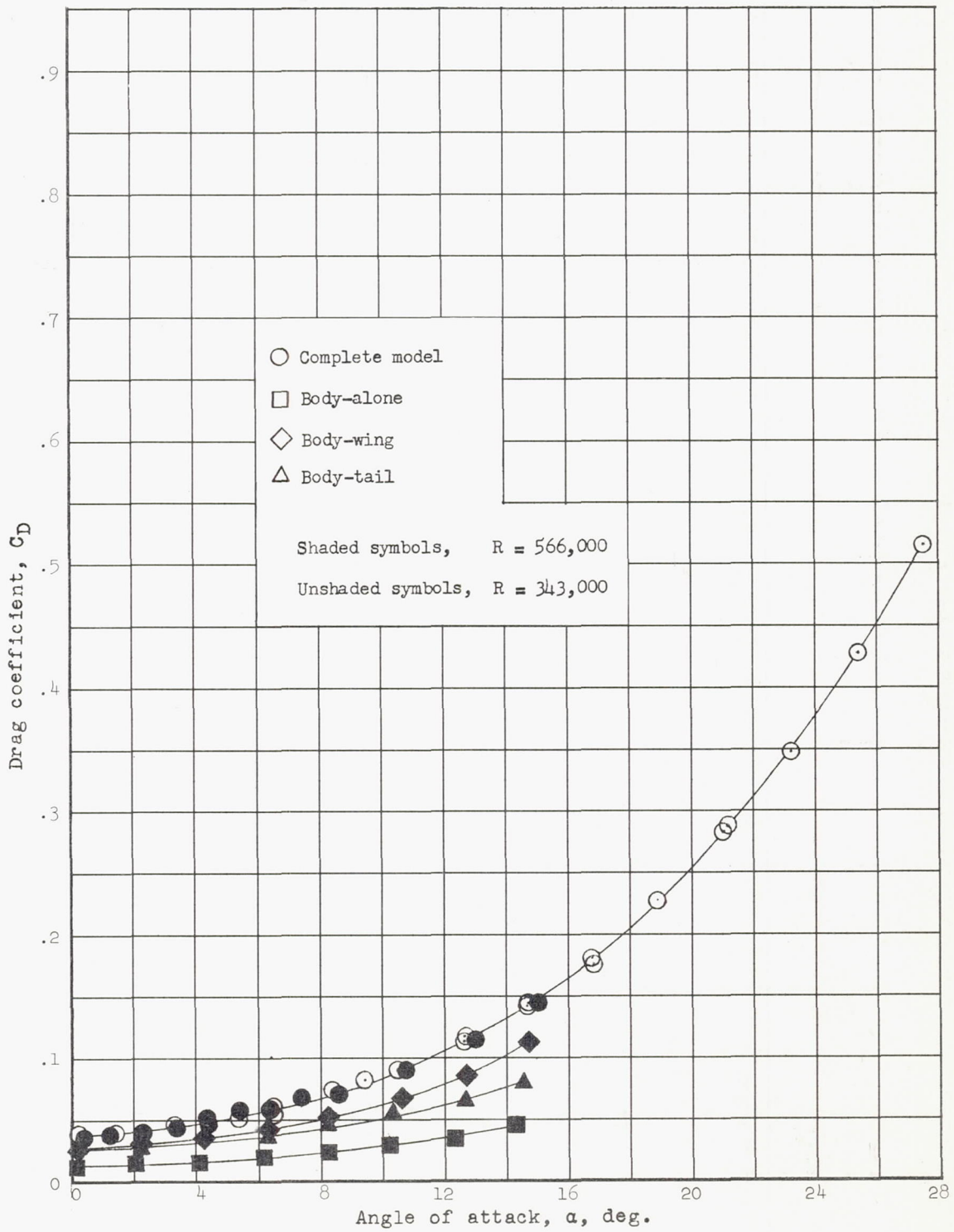

Figure 9.- The variations of the drag coefficient with angle of attack for the model and its components. M = 6.86.

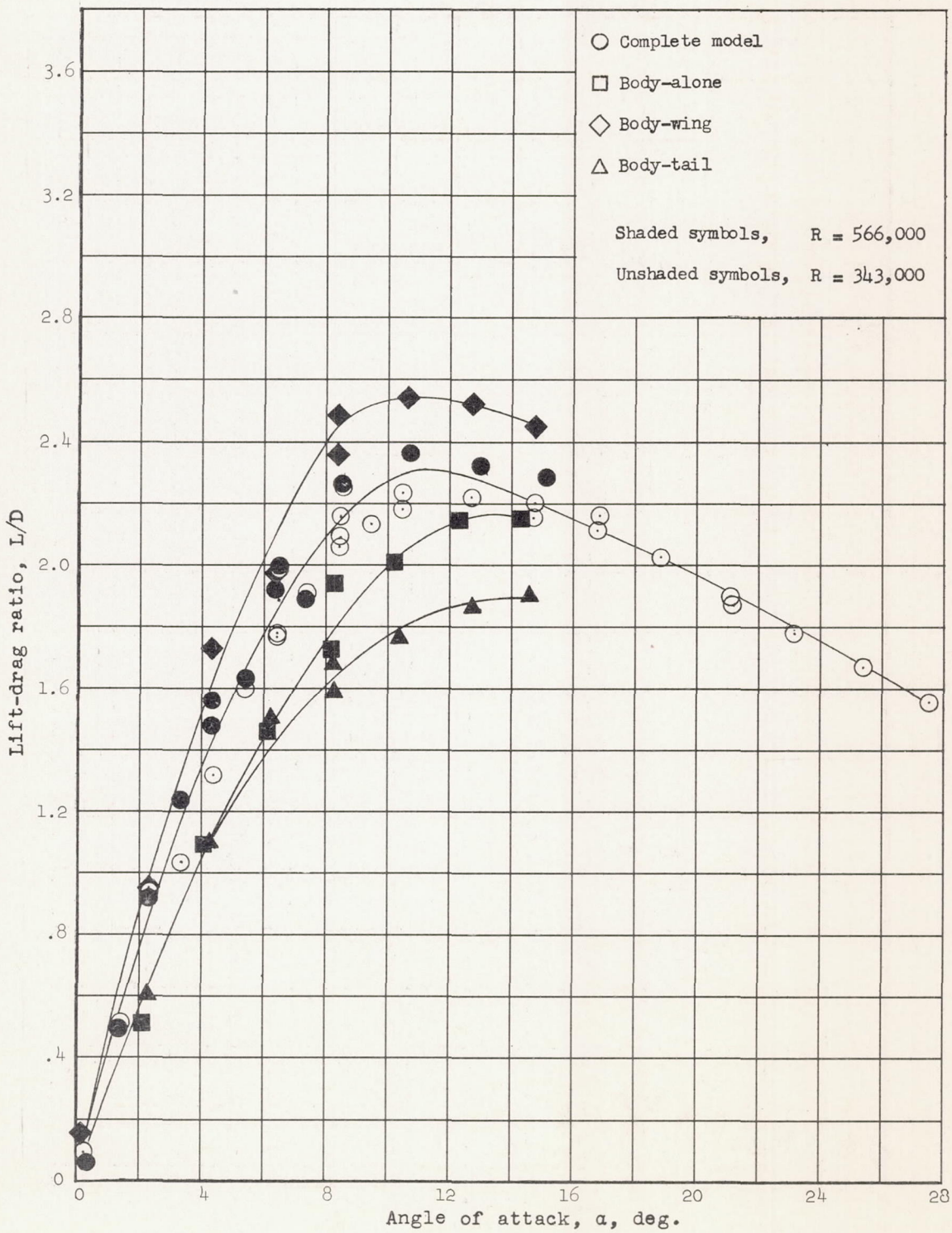

Figure 10.- Variation of lift-drag ratio with angle of attack for model and its components. M = 6.86.

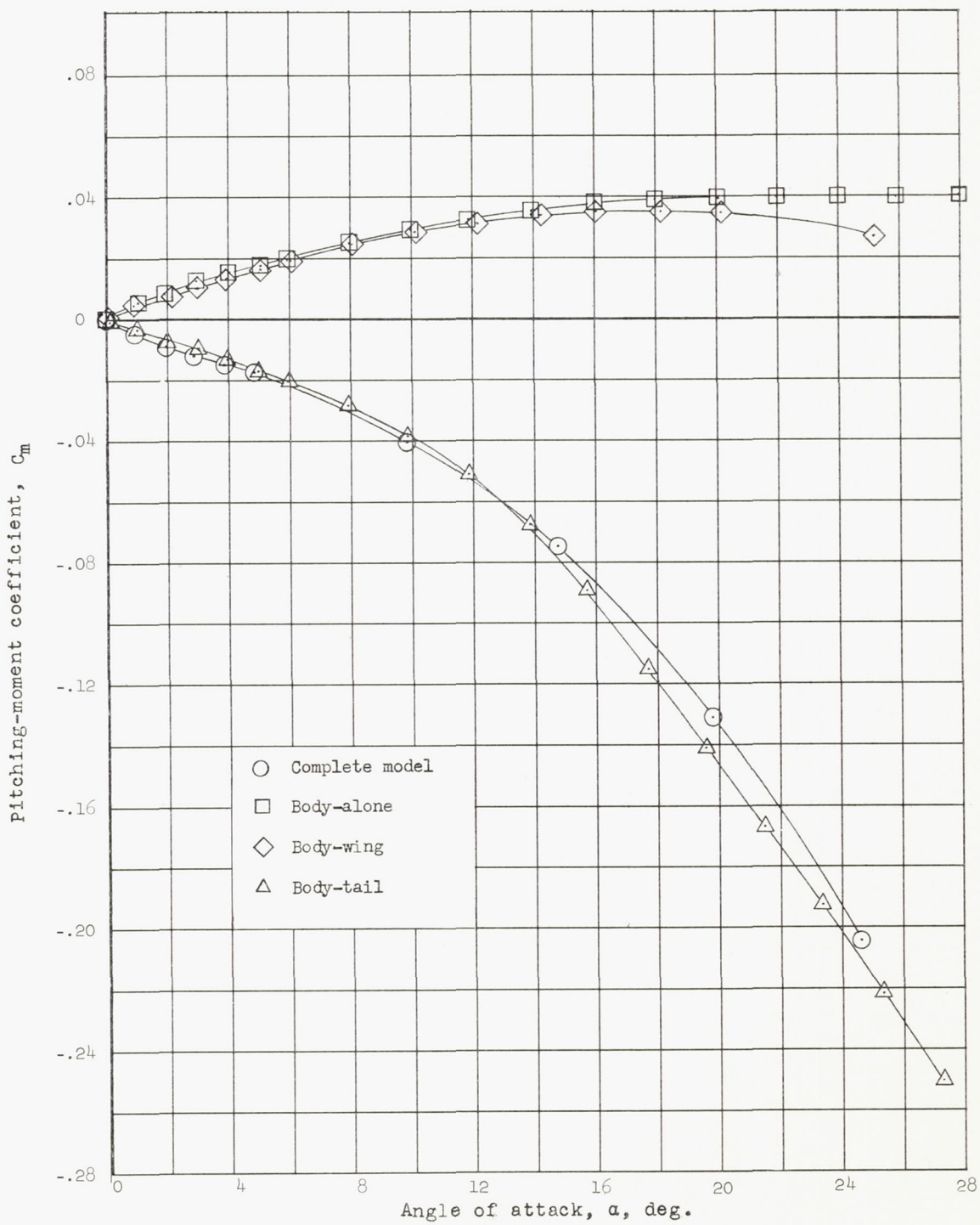

Figure 11.- Variation of pitching-moment coefficient with angle of attack for model and its components. M = 6.86; R = 343,000.

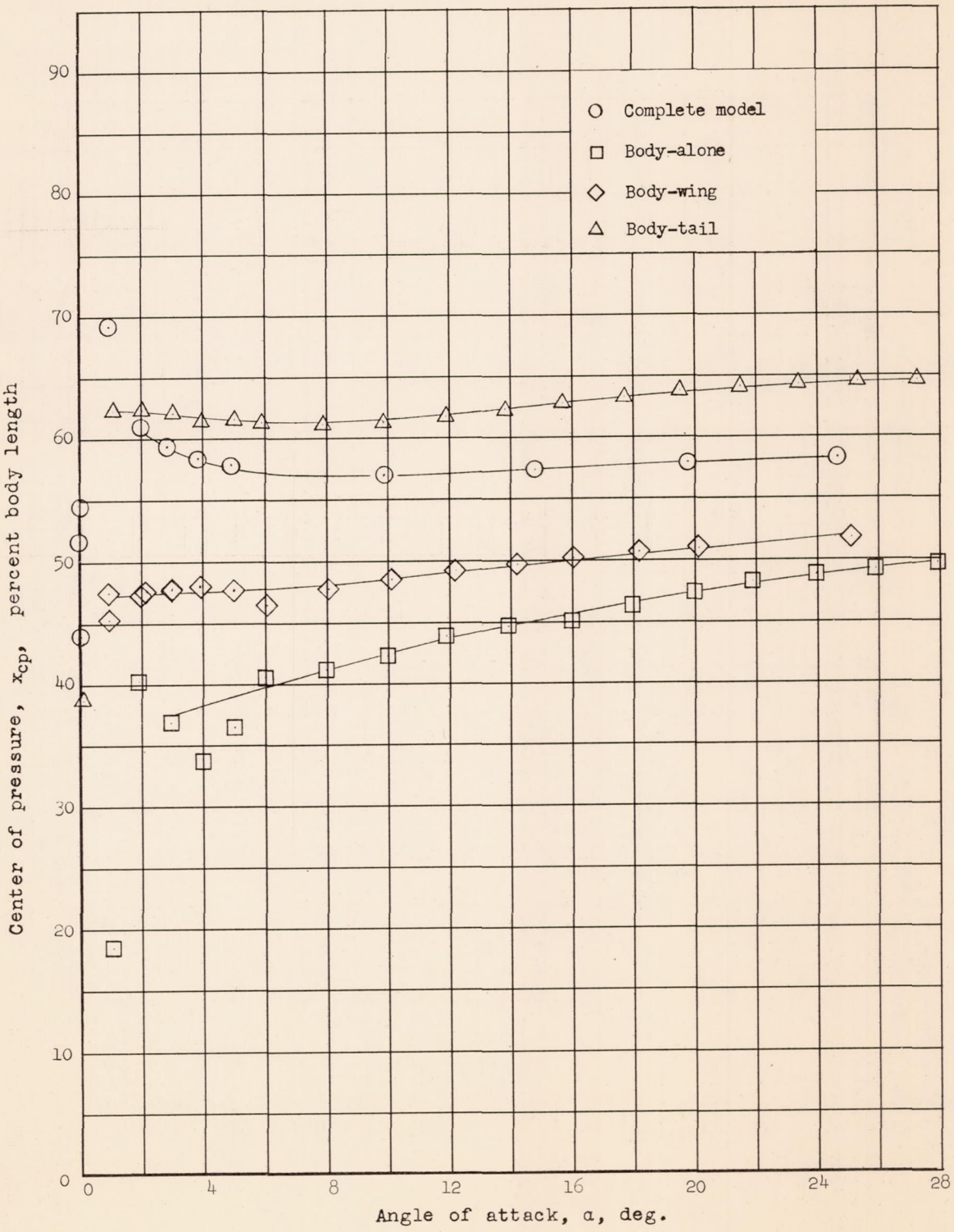

Figure 12.- Variation of center-of-pressure location with angle of attack for model and its components. M = 6.86; R = 343,000.

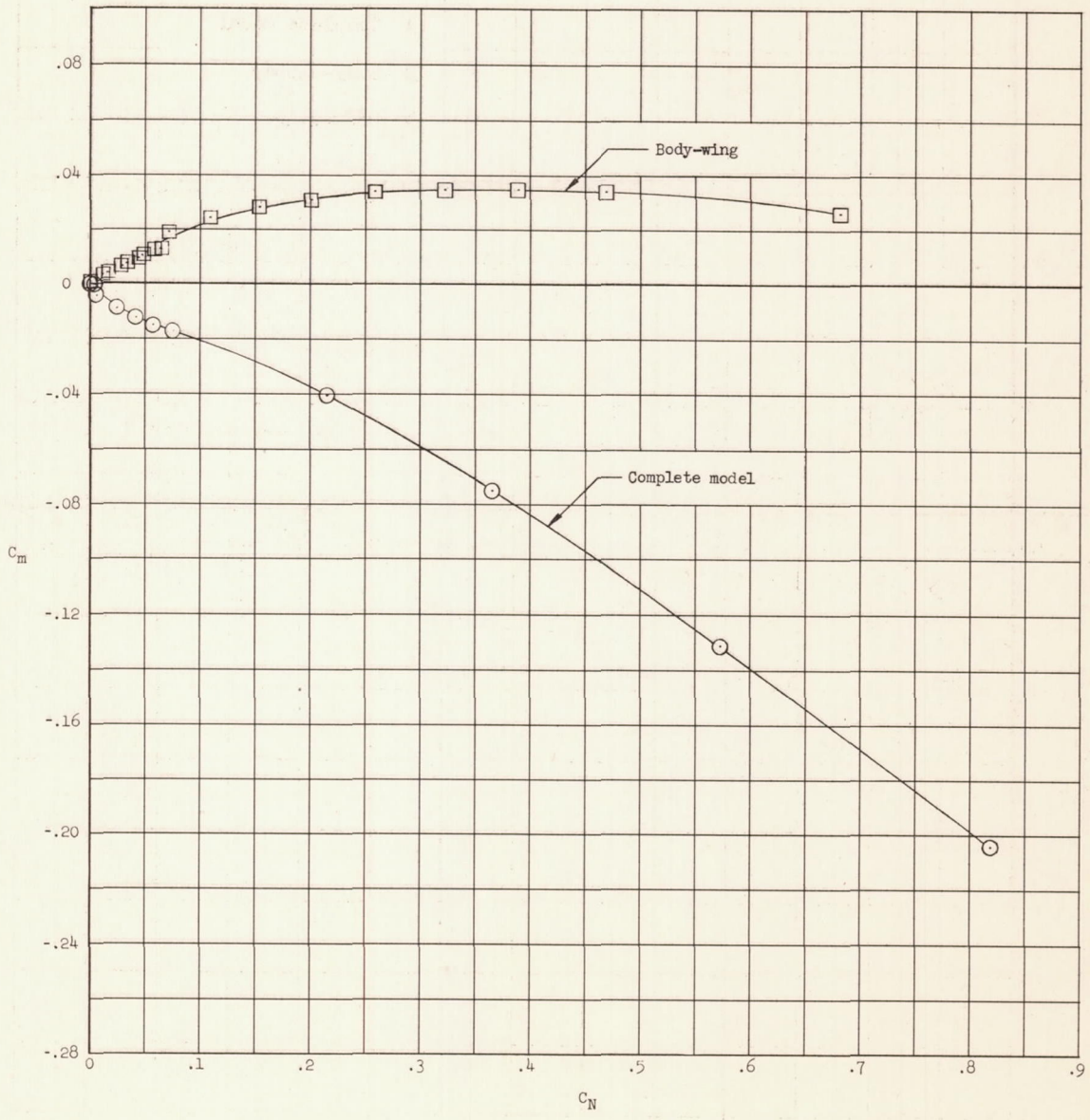

Figure 13.- Variations of pitching-moment coefficient with normal-force coefficient for complete model and body-wing configuration. M = 6.86; R = 343,000.

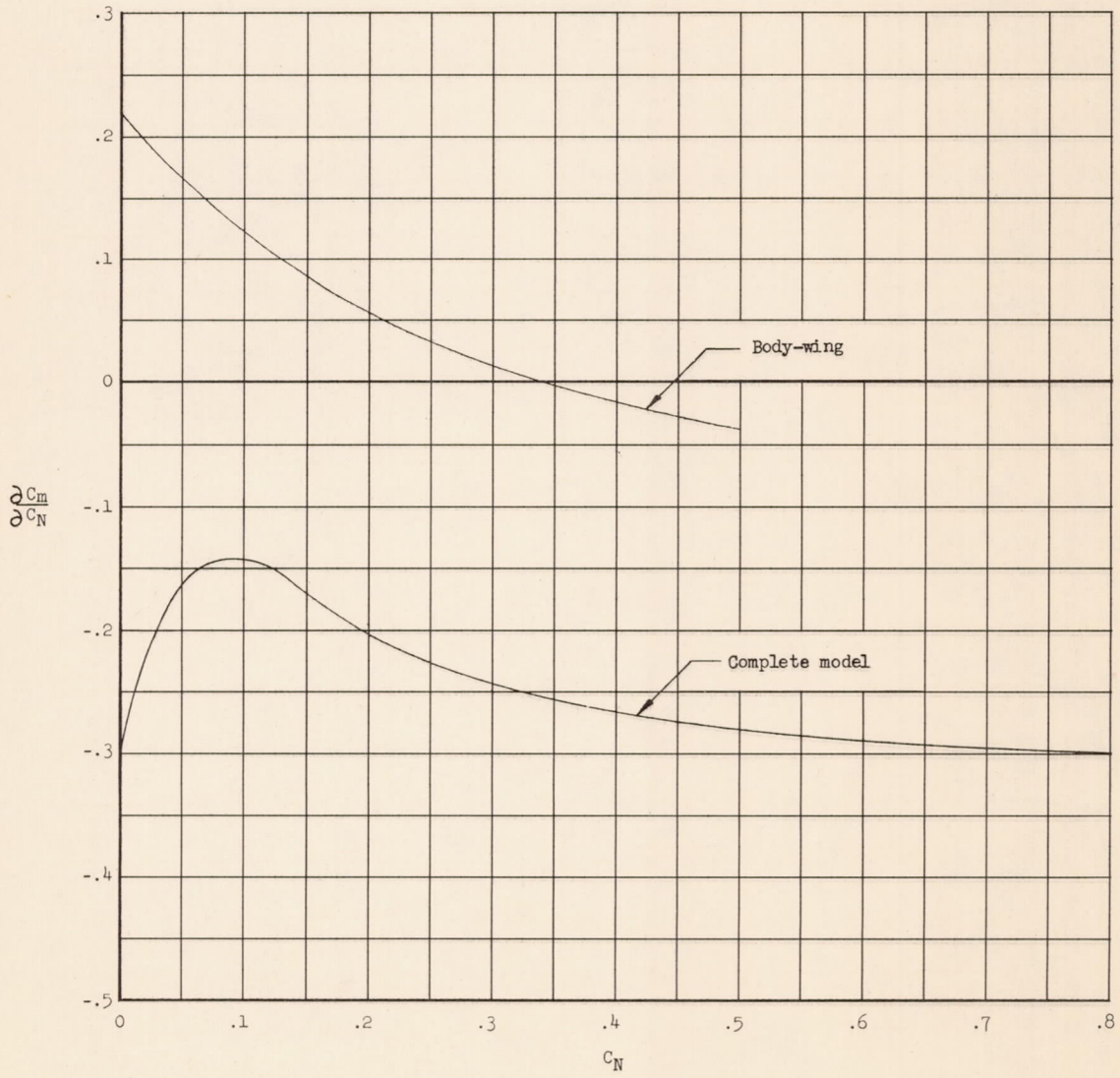

Figure 14.- Variation of the static-longitudinal-stability parameter $\frac{\partial C_m}{\partial C_N}$ with normal-force coefficient for complete model and body-wing configuration. M = 6.86; R = 343,000.

NACA-Langley - 1-18-55 - 325